Transactions of the Materials Research Society of Japan 30[3] 707-710 (2005)

Photoelectrochemical Properties of Nano-Structured Polymer Ultrathin Films on Conductive Substrates

Hideo Ohkita, Kuniaki Sakai, and Shinzaburo Ito*
Department of Polymer Chemistry, Graduate School of Engineering, Kyoto University
Katsura, Nishikyo-ku, Kyoto 615-8510, Japan
Fax: 81-75-383-2617, e-mail: ohkita@photo.polym.kyoto-u.ac.jp

Fluorescence quenching and photocurrent generation were studied by using nano-structures of ultrathin polymer films on conductive substrates. The multilayered nano-structures enable one to control the separation distance d between carbazole (Cz) moiety and a conductive substrate on a nanometer scale by changing the number of spacing layers. Fluorescence quenching of the Cz moiety by an ITO substrate decreased as the separation distance increased and was negligible around d = 12 nm. This long-range quenching was explained by the energy transfer. The theoretical prediction reproduced the distance dependence of the fluorescence quenching of Cz* in the excited state by the ITO substrate. On the other hand, the fluorescence of Cz on an Au electrode was quenched even at d = 12 nm. This quenching is probably due to larger spectral overlap between the fluorescence of Cz and the absorption of the conductive substrate. To discuss the effect of the fluorescence quenching on photocurrent generation, we fabricated two types of heterostructured ultrathin polymer films by using Cz and ferrocene (Fc) polymers: ITO/Cz/Fc and ITO/Fc/Cz. A larger anodic photocurrent was observed for the ITO/Fc/Cz|MV system while a smaller cathodic photocurrent was observed for the ITO/Cz/Fc|TEOA system where Cz* in the excited state was quenched by the ITO substrate.

Key words: fluorescence quenching; ultrathin polymer films; energy transfer; conductive substrates, photocurrent

1. INTRODUCTION

Ultrathin polymer films are one of the most attractive materials for constructing layered nano-structures. The ultrathin polymer films can be fabricated in a simple and easy way such as Langmuir–Blodgett (LB) method [1] and layer-by-layer deposition technique [2]. In particular, polymer LB films have been used as a useful nano-ruler to evaluate photophysical elementary processes quantitatively, because the interlayer distance can be controlled with nanometer-scale precision. For example, the monolayer thickness of polyimide LB films is as thin as 0.4 nm, which is comparable to the thickness of aromatic molecules. Taking these advantages into consideration, we previously studied excitation energy transfer [3–5], electron transfer [6], and two-photon ionization [7,8] in multilayered ultrathin polymer LB films.

Quenching of the excited state of a fluorescent dye due to coupling to a conductive electrode was a topic of study in the 1960s [9]. The theoretical description has been presented in an excellent paper by Chance et al. [10]. Even now, this issue is attracting much attention in various fields. For example, the efficiency of organic electroluminescence devices is considered to be crucially affected by the thin metal layer [11,12]. The metal quenching also adversely affects the performance of organic solar cells. Forrest at el. [13] incorporated an exciton-blocking layer between an acceptor layer and a cathodic metal in organic solar cells to avoid exciton quenching at the cathode.

Here we studied the dependence of fluorescence quenching of aromatic molecules on the separation distance between the molecules and a conductive substrate. The separation distance varied from 1 to 12 nm by changing the number of spacing layers in the LB films. On the basis of the quenching experiment, we discuss photocurrent generation in two types of heterostructured ultrathin polymer films.

2. EXPERIMENTAL

2.1 Materials

Poly[2-(9-carbazolyl)ethyl methacrylate-*co*-isobutyl methacrylate] (P(Cz-iBMA)) and poly(ferrocenylmethyl methacrylate-*co*-isobutyl methacrylate) (P(Fc-iBMA)) were synthesized by random copolymerization of isobutyl methacrylate with 2-(9-carbazolyl)ethyl methacrylate and isobutyl methacrylate with ferrocenylmethyl methacrylate, respectively [5]. The mole fraction of Cz or Fc moiety was estimated to be ca. 15 mol % for P(Cz-iBMA) and ca. 11 mol % for P(Fc-iBMA) by absorption measurement. Poly(vinyl pentanal) (PVPe) was synthesized by acetalization of poly(vinyl alcohol) (PVA, Wako Pure Chem. Ind., Ltd., degree of polymerization = 2000) with 1-pentanal (Wako Pure Chem. Ind., Ltd.). Detailed synthetic procedures of PVPe have been described elsewhere [7].

2.2 Preparation of LB films

Three kinds of substrates were used: quartz (10 × 40 × 1 mm^3), ITO (10 × 40 × 1 mm^3, 10 Ω per square), and Au-coated quartz (10 × 40 × 1 mm^3, thickness of Au = 50 nm). The quartz substrate was cleaned by immersion in SCAT 20X-N (Nacalai) and then into 30 wt% H_2O_2 / conc. H_2SO_4 (3 : 7 (v/v)) for 1 day. The ITO substrate was thoroughly cleaned by immersion in SCAT 20X-N and successive ultrasonic treatments in toluene, acetone, and ethanol for 20 min, followed by rinsing with boiling ethanol for 20 min. Subsequently,

the ITO substrate was boiled at 70 °C in a mixture of H_2O / 30 wt% H_2O_2 / 25% NH_3 aq. (5 : 1 : 1 (v/v)) for 20 min. The Au-coated quartz substrate was prepared by thermal deposition of Cr (5 nm) and Au (50 nm) on a cleaned quartz plate. These substrates were dried with nitrogen gas. A benzene solution of each polymer (10^{-3} unit mol L^{-1}) was spread on pure water using a trough (Kenkosha Model SI-1) equipped with a Wilhelmy-type film balance. The water used as subphase was purified by deionization, distillation, and passing through the filtration system (Barnstead Nanopure II). The LB film was deposited at a surface pressure of 8 mN m^{-1} for P(Cz-iBMA) and P(Fc-iBMA), and 20 mN m^{-1} for PVPe at 20 °C with a dipping speed of 2 mm min^{-1}. The LB films were dried overnight in a desiccator at room temperature. Thickness of the monolayer is 1.06 nm for P(Cz-iBMA) and P(Fc-iBMA), and 0.90 nm for PVPe [7].

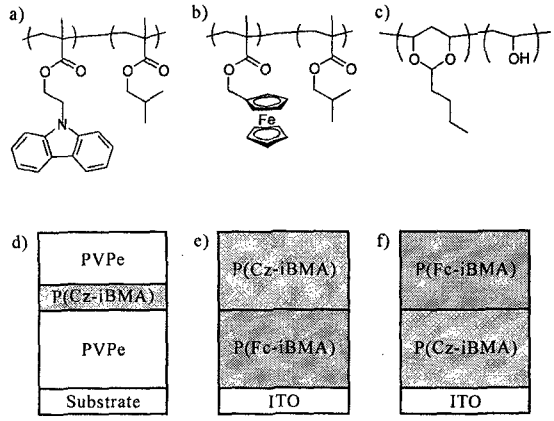

Fig. 1. Top: chemical structures of a) P(Cz-iBMA), b) P(Fc-iBMA), and c) PVPe. Bottom: layer structures of LB films used for d) fluorescence quenching measurement and for e, f) photocurrent measurement.

Each polymer was deposited as a Y or Z-type LB film with a high transfer ratio both in the up and down modes. Figure 1d shows the layer structure of the LB film on ITO, Au-coated quartz, and quartz substrates, which are abbreviated as ITO(n), Au(n), and Q(n), respectively, where n is the number of PVPe spacing layers. The LB films used for the fluorescence quenching experiment were fabricated on a substrate in the following sequence: (1) n (0, 1, 3, 5, 7, 9, 13 for ITO(n); 7, 13 for Au(n); 13 for Q(n)) layers of PVPe as the spacing layers, (2) 1 layer of P(Cz-iBMA) as the chromophore layer, (3) 2 layers of PVPe as the protection layers. The LB films used for the photocurrent generation experiment were fabricated on the ITO substrate in the following sequence: (1) 3 layers of P(Fc-iBMA), (2) 3 layer of P(Cz-iBMA) and also in reverse order. Figures 1e and 1f show the layer structures, which are abbreviated as ITO/Fc/Cz and ITO/Cz/Fc, respectively.

2.3 Measurements.

UV–visible absorption spectra were measured with a spectrophotometer (Hitachi U-3500). Steady-state fluorescence spectra were recorded with a fluorescence spectrophotometer (Hitachi F-4500). Fluorescence decay was measured by the time-correlated single-photon-counting method. The excitation light source was third harmonic pulses (295 nm) generated from a mode-locked Ti: sapphire laser (Spectra-Physics, Tsunami 3950) that was pumped by an Ar^+ laser (Spectra-Physics, BeamLok 2060). The fluorescence emission was detected with a photomultiplier tube (Hamamatsu Photonics, R3234) through a monochromator (Ritsu, MC-10N) set at 370 nm with an optical cut-filter (UV-34) for the excitation light. The details of this apparatus have been described elsewhere [14]. The total instrument response function has an FWHM of ca. 750 ps. The decay data were fitted with a sum of exponential functions that were convoluted with the instrument response function by the nonlinear least-squares method.

Photocurrent generation in the LB films was measured with a potentiostat (Perkin Elmer, 273A), a three-electrode electrochemical cell with a 0.95-cm^2 window for mounting the ITO substrate as a working electrode, and 500-W xenon lamp with optical cut-filters (UV-32, UVD-33S, IRQ-80). The reference and counter electrodes were an Ag/AgCl electrode with a saturated KCl aqueous solution and a Pt net, respectively. The electroyte solution was a 1.0 M $NaClO_4$ aqueous solution. Triethanolamine (TEOA) and methyl viologen (MV^{2+}) were used as sacrifice reagents.

3. RESULTS AND DISCUSSION

3.1 Steady-state fluorescence spectra

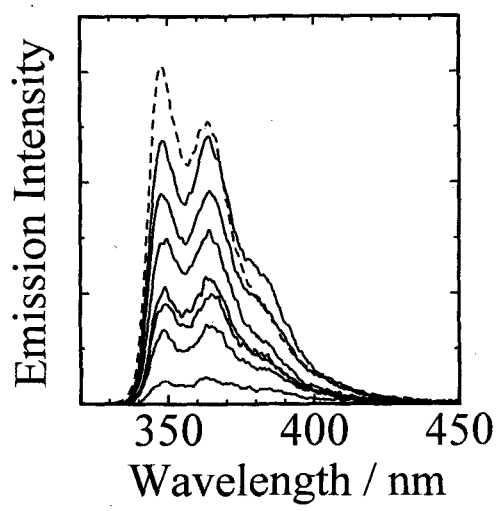

Fig. 2. Fluorescence spectra of Cz in the LB films. From top to bottom: Q(13) (broken line), ITO(n) n = 13, 9, 7, 5, 3, 1, 0 (solid lines).

To discuss the dependence of fluorescence quenching on the separation distance between aromatic molecules and a conductive electrode, we measured the fluorescence intensity of the LB film with various numbers of spacing layers as shown in Figure 1d. Figure 2 shows the fluorescence spectra of Cz in ITO(n). The fluorescence intensity of ITO(n) increased with the increase in the number of spacing layers n and that of ITO(13) became close to that of Q(13) where a Cz layer is separated with 13 layers of PVPe from a quartz substrate. The separation distance between the Cz layer and a substrate with 13 layers of PVPe is roughly estimated to be about 12 nm because the monolayer

thickness is 0.90 nm for PVPe and 1.06 nm for P(Cz-iBMA). This finding shows that Cz* in the LB film is no longer quenched when the Cz layer is separated from the ITO substrate over ~10 nm. On the other hand, Figure 3 shows the fluorescence spectra

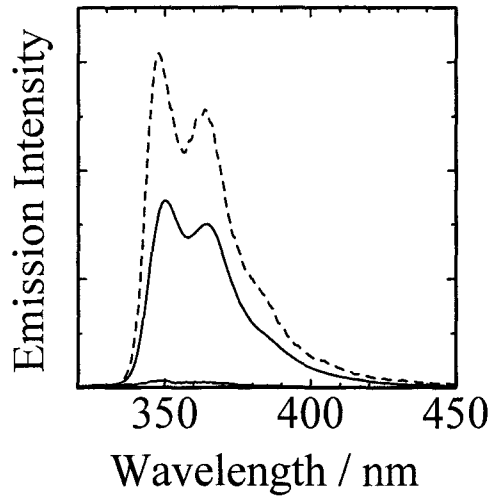

Fig. 3. Fluorescence spectra of carbazole moiety in the LB films. From top to bottom: Q(13), Au(n) n = 13 and 7.

of Cz in Au(n) where the Cz layer is separated by n layers of PVPe from an Au-coated quartz substrate. The fluorescence intensity of Au(n) was significantly quenched at n = 7 and did not recover even at n = 13 whereas that of ITO(13) was close to that of Q(13). In other words, Cz* in the excited state is still quenched even when it is separated from the Au-coated substrate over ~10 nm. The quenching distance is too long to be ascribed to electron transfer between the Cz layer and conductive substrates. In general, electron transfer from an aromatic molecule in the excited state will occur within a separation distance of 1–2 nm [15]. Therefore, the quenching mechanism is probably ascribed to energy transfer from Cz* in the excited state to conductive substrates.

3.2 Fluorescence decay

To discuss the fluorescence quenching quantitatively, we measured the fluorescence decay $I(t)$ of Cz in ITO(n), Au(n), and Q(13) by the time-correlated single-photon-counting method. Figure 4 shows the fluorescence decays of Cz in ITO(n) with n = 0 – 13 (closed circles) and Q(13) (open circles). Fluorescence lifetime was evaluated from the fitting analysis by the nonlinear least-square method. The fluorescence decay $I(t)$ was well fitted with a sum of two exponentials $I(t) = A_1 \exp(-t/\tau_1) + A_2 \exp(-t/\tau_2)$. The averaged fluorescence lifetime $<\tau>$ was calculated by $<\tau> = \Sigma A_i \tau_i / \Sigma A_i$. Similar to the results for the fluorescence spectra, the lifetimes $<\tau>$ of Cz* in the excited state in ITO(n) also increased with increases in the number of spacing layers n and $<\tau>$ of Cz* in ITO(13) became close to $<\tau_0>$ in Q(13). These results prove that the decrease in fluorescence intensity is due to quenching of Cz* in the excited state.

The apparent quenching rate k_Q was calculated by

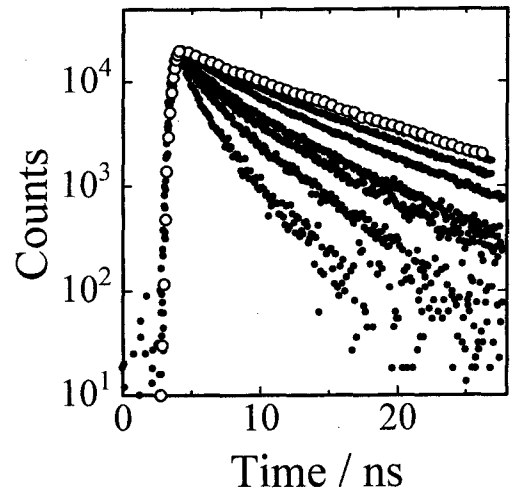

Fig. 4. Fluorescence decays of carbazole moiety in the LB films. From top to bottom: Q(13), ITO(n) n = 13, 9, 7, 5, 3, 1, 0.

$<\tau>^{-1} - <\tau_0>^{-1}$ where $<\tau_0>$ is the averaged lifetime of Cz* in Q(13). With increases in the number of spacing layers n, the quenching rate k_Q was reduced to $< 5 \times 10^6$ s^{-1} for ITO(13), which was two orders of magnitude less than 5.6×10^8 s^{-1} for ITO(0). This finding shows that the excited state of Cz formed on the ITO substrate is deactivated within a nanosecond through non-radiative processes. To make use of the excitation energy, therefore, we have to design the layer structure for reducing the deactivation process or for promoting the rapid charge injection into ITO enough to compete with the deactivation process.

3.3 Separation distance dependence of fluorescence quenching

Figure 5 shows the dependence of the fluorescence quenching on the separation distance between the Cz layer and the ITO substrate. The open circles show the steady-state fluorescence intensity of ITO(n) normalized by that of Q(13). The closed circles represent the lifetime of Cz* in ITO(n) normalized by that in Q(13). Both of them were in good agreement with each other, suggesting that the same phenomenon was surely observed by the fluorescence quenching and the fluorescence decay measurements independently. The solid curve is the theoretical prediction calculated in accordance with Chance et al. [10], which well agreed with the experimental plots. In the theory, the fluorescence quenching rate is proportional to d^{-3}, because the separation distance d is enough shorter than the thickness of the ITO layer (~ 200 nm). Consequently, we conclude that the mechanism of the fluorescence quenching is the energy transfer from Cz* in the excited state to the ITO substrate. On the other hand, the open and closed squares in the figure represent the normalized fluorescence intensity I/I_0 and the normalized lifetime $<\tau>/<\tau_0>$ of Cz* in Au(n), respectively. The broken curve is a theoretical one. Both I/I_0 and $<\tau>/<\tau_0>$ for Au(n) were smaller than those for ITO(n), suggesting that Cz* in the excited state was still quenched even at n = 13 (d ~ 12 nm). The apparent quenching rate k_Q for Au(7) is about 10 times

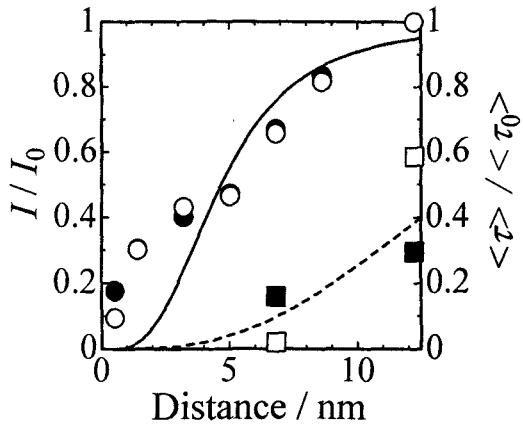

Fig. 5. Separation distance dependence of I/I_0 and $\langle\tau\rangle/\langle\tau_0\rangle$ for Au(n) and ITO(n). Left axis: open circles are I/I_0 for ITO(n) and open squares are I/I_0 for Au(n); Right axis: closed circles are $\langle\tau\rangle/\langle\tau_0\rangle$ for ITO(n) and closed squares are $\langle\tau\rangle/\langle\tau_0\rangle$ for Au(n).

faster than that for ITO(7). This difference is probably attributed to the spectral overlap of the fluorescence of Cz with the absorption of conductive substrates. The Au-coated substrate has broad absorption in the visible region while the ITO plate has absorption only in the UV region.

3.4 Photocurrent response

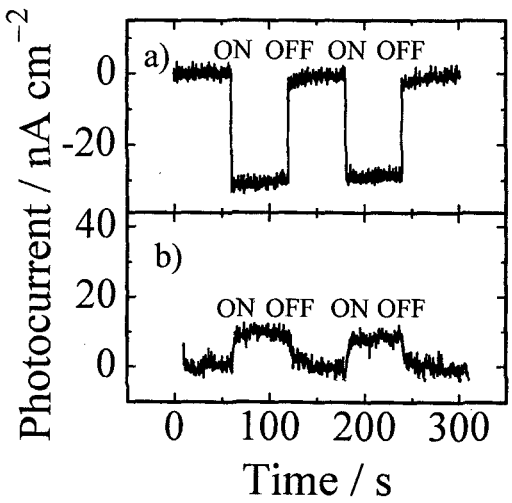

Fig. 6. Photocurrent generation in the LB films under irradiation at a light intensity of 13 mW cm^{-2}: a) ITO/Fc/Cz|MV^{2+}, b) ITO/Cz/Fc|TEOA.

Figure 6 shows photocurrent generation in the two types of heterostructured LB films under the photoirradiation. One is the layer structure shown in Figure 1e with 30 mM MV^{2+} (ITO/Fc/Cz|MV^{2+}). The other is the layer structure shown in Figure 1f with 30 mM TEOA (ITO/Fc/Cz|TEOA). For ITO/Fc/Cz|MV^{2+}, cathodic photocurrents of ~30 nA cm^{-2} were repeatedly observed in response to the on/off light switching. For ITO/Cz/Fc|TEOA, on the other hand, anodic photocurrents were repeatedly observed. The direction of photocurrent results from potential gradients designed in each LB film, suggesting that the photocurrent was controlled by the layered nano-structures. The anodic photocurrent in ITO/Cz/Fc|TEOA was one third of the cathodic photocurrent in ITO/Fc/Cz|MV^{2+}. In ITO/Cz/Fc|TEOA, Cz* in the excited state is to some extent quenched by the ITO substrate because the separation distance between the Cz layer and the ITO substrate is shorter than that in ITO/Fc/Cz|MV^{2+}. This may be one of the reasons for the decrease in photocurrent generation.

4. CONCLUSIONS

Aromatic molecules in the excited state on ITO substrate were quenched by long-range energy transfer. The fluorescence quenching rate was inversely proportional to the cube of the separation distance d between the aromatic molecule and the ITO substrate. Compared with the ITO substrate, the fluorescence of aromatic molecules on the Au substrate was significantly quenched. A larger photocurrent was generated for the layered nano-structures where aromatic molecules are separated from the ITO substrate by the spacing layers.

ACKNOWLEDGMENTS

This work was partly supported by the Integrative Industry–Academia Partnership (IIAP) including Kyoto University, Nippon Telegraph and Telephone Corporation, Pioneer Corporation, Hitachi, Ltd., Mitsubishi Chemical Corporation and Rohm Co., Ltd and by the 21st Century COE program, COE for a United Approach to New Materials Science.

REFERENCES

[1] R. H. Tredgold, *J. Phys. D, Appl. Phys.*, **15**, L55–58 (1982).
[2] G. Decher, *Thin Solid Films*, **210**, 831–835 (1992).
[3] S. Ohmori, S. Ito, M. Yamamoto, *Macromolecules*, **23**, 4047–4053 (1990).
[4] S. Ohmori, S. Ito, M. Yamamoto, *Macromolecules*, **24**, 2377–2384 (1991).
[5] S. Ito, S. Ohmori, M. Yamamoto, *Macromolecules*, **25**, 185–191 (1992).
[6] H. Ohkita, T. Ogi, R. Kinoshita, S. Ito, M. Yamamoto, *Polymer*, **43**, 3571–3577 (2002).
[7] H. Ohkita, H. Ishii, S. Ito, M. Yamamoto, *Chem. Lett.*, **2000**, 1092–1093.
[8] H. Ohkita, H. Ishii, T. Ogi, S. Ito, M. Yamamoto, *Radiat. Phys. Chem.*, **60**, 427–432 (2001).
[9] K. H. Drexhage, "Progress in Optics XII", Ed. By E. Wolf, North-Holland, Amsterdam (1974).
[10] R. R. Chance, A. Prock, R. Silbey, "Advances in Chemical Physics", Eds. I. Prigogine, S. R. Rice, Wiley, New York (1978).
[11] V. Choong, Y. Park, Y. Gao, T. Wehrmeister, K. Müllen, B. R. Hsieh, C. W. Tang, *Appl. Phys. Lett.*, **69**, 1492–1494 (1996).
[12] H. Becker, A. Lux, A. B. Holmes, R. H. Friend, *Synth. Met.*, **85**, 1289–1290 (1997).
[13] P. Peumans, A. Yakimov, S. R. Forrest, *J. Appl. Phys.*, **93**, 3693–3723 (2003).
[14] H. Ohkita, S. Ito, M. Yamamoto, Y. Tohda, K. Tani, *J. Phys. Chem. A*, **106**, 2140–2145 (2002).
[15] K. Nagai, T. Nishijima, N. Takamiya, M. Tada, M. Kaneko, *J. Photochem. Photobiol. A: Chem.*, **92**, 47–51 (1995).

(Received January 6, 2005; Accepted April 28, 2005)